

STCMOT: Spatio-Temporal Cohesion Learning for UAV-Based Multiple Object Tracking

1st Jianbo Ma

National Key Laboratory of Optical Field
Manipulation Science and Technology
Key Laboratory of Optical Engineering
Institute of Optics and Electronics
University of Chinese Academy of Sciences
Chengdu, China
majianbo22@mails.ucas.ac.cn

2nd Chuanming Tang

Institute of Optics and Electronics
University of Chinese Academy of Sciences
Chengdu, China
tangchuanming19@mails.ucas.ac.cn

3rd Fei Wu

Pattern Recognition Lab
Department of Computer Science
Friedrich-Alexander-Universität
Erlangen-Nürnberg
Erlangen, Germany
river.wu@fau.de

4th Can Zhao

Institute of Optics and Electronics
University of Chinese Academy of Sciences
Chengdu, China
zhaocan22@mails.ucas.ac.cn

5th Jianlin Zhang*

Key Laboratory of Optical Engineering
Institute of Optics and Electronics
Chengdu, China
jlin@ioe.ac.cn

6th Zhiyong Xu

Key Laboratory of Optical Engineering
Institute of Optics and Electronics
Chengdu, China
xuzhiyong@ioe.ac.cn

Abstract—Multiple object tracking (MOT) in Unmanned Aerial Vehicle (UAV) videos is important for diverse applications in computer vision. Current MOT trackers rely on accurate object detection results and precise matching of target re-identification (ReID). These methods focus on optimizing target spatial attributes while overlooking temporal cues in modelling object relationships, especially for challenging tracking conditions such as object deformation and blurring, etc. To address the above-mentioned issues, we propose a novel Spatio-Temporal Cohesion Multiple Object Tracking framework (STCMOT), which utilizes historical embedding features to model the representation of ReID and detection features in a sequential order. Concretely, a temporal embedding boosting module is introduced to enhance the discriminability of individual embedding based on adjacent frame cooperation. While the trajectory embedding is then propagated by a temporal detection refinement module to mine salient target locations in the temporal field. Extensive experiments on the VisDrone2019 and UAVDT datasets demonstrate our STCMOT sets a new state-of-the-art performance in MOTA and IDF1 metrics. The source codes are released at <https://github.com/ydhcg-BoBo/STCMOT>.

Index Terms—Multiple Object Tracking, Spatio-Temporal Model, Unmanned Aerial Vehicle

I. INTRODUCTION

The goal of multiple object tracking (MOT) is to recognize various designated target categories in video sequences. In recent years, the MOT algorithms for unmanned aerial vehicle (UAV) videos have captured the interest of researchers. Its primary task lies in effectively tracking multiple objects within UAV views. However, with the distance between the objects and the UAV camera, objects are typically small and prone to blurring. This results in many challenging attributes for the UAV-based MOT task [1]. Unlike stationary shooting,

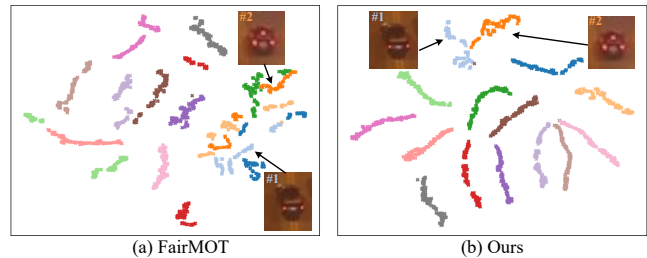


Fig. 1. T-SEN projection of ReID embeddings for the 15 tracked targets in the UAVDT-M1007 video. STCMOT shows a more discriminative embedding representation compared with the baseline FairMOT, even in the cases where targets #1 and #2 have similar appearances during nighttime.

the dynamic motion of the UAV introduces continuous object position changes and multi-dimensional scaling issues related to the ground objects. As a result, the performance of UAV tracking is easily impaired by interference from similar distractors and occlusions.

To address these challenges, previous works [2], [3] mainly utilize the two-stage tracking framework to enhance tracking capability. They first introduce a detection model to identify the objects' positions. Subsequently, the motion information and re-identification (ReID) embeddings of object candidates are established and connected to complete the matching. Despite the remarkable tracking performance from these two-stage trackers [2]–[5], using the respective network for object detection and embedding extraction results in considerable storage cost and resource consumption [6]. To this end, the one-shot tracking algorithms [7]–[9] integrate the detection branch and the ReID branch into a unified framework for balancing tracking performance and speed. For example, FairMOT [8] merges an additional ReID branch into the

* Corresponding author

CenterNet [10]. It takes a single-frame image as input and simultaneously produces the detected target and corresponding embedding features. This streamlined tracking framework can simplify the tracking process and thus is more suitable for real-world object tracking in UAV videos.

Additionally, propelled by the advancement of deep convolutional networks, some works [11]–[14] use enhanced deep features in the one-shot tracking framework and achieve higher performance. To obtain pixel-wise relations at multiple feature levels, Wu et al. [11] firstly design a pyramid transformer encoder for the detection branch, then a channel-wise transformer encoder which equipped with the pyramid fusion network [12] is used to enhance the ReID branch. At the same time, Yu et al. [13] propose a guided transformer encoder to emphasize global semantic information. Liang et al. [14] introduce a scale-aware attention network to alleviate object semantic misalignments. In addition to enhancing the feature representation from global and local spatial perspectives, Liu et al. [15] model the temporal relationship of ID features and propose an ID feature update module to adapt to appearance changes in various UAV views. However, the multiple object spatio-temporal cues from the detection branch have not yet been seriously considered in these works, which inspires us to construct a spatio-temporal interaction model between detection and ReID branches to handle complex tracking scenarios. E.g., object deformation and blurring.

In this paper, we propose a unified spatio-temporal cohesion learning network for MOT in UAV-captured videos, termed STCMOT. STCMOT extends the salient ReID embeddings from the historical frame to the current frame, optimizing and enhancing both detection and ReID branches. In particular, we first introduce a temporal embedding boosting module. It couples the ReID feature map from adjacent frames and generates a channel-wise descriptor to highlight the discriminability of individual embedding. Secondly, a temporal detection refinement module is built upon the inherent continuity of individual embedding in video sequences. This module regards each previous target embedding as a query, facilitating information interactions with the current ReID feature map during one-shot network training.

In this way, the object spatio-temporal coupling strategy can optimize the detection and ReID branches at the same time, thus strengthening the network association capability and reducing tracking failures. The experimental results demonstrate that the proposed method surpasses the current state-of-the-art trackers in MOTA and IDF1 metrics. Overall, the main contributions of this work can be summarized in the following three aspects:

- We emphasize the importance of introducing the ReID feature map from successive frames in MOT. A temporal embedding boosting module (named TEBM) is proposed to improve the specificity of individual embedding at the feature channel level.
- We propose a temporal detection refinement module named TDRM. It is designed to leverage the object moving continuity and trajectory embedding for refining

fine-grained object position and enhancing detection performance.

- With the proposed spatio-temporal semantic embedding cohesion strategy, STCMOT achieves new state-of-the-art performance on both VisDrone2019 and UAVDT benchmarks.

II. METHODOLOGY

A. Overall Framework

As shown in Fig. 2, STCMOT can be divided into three parts: an adjacent frame feature extractor, a temporal embedding boosting module (TEBM), and a temporal detection refinement module (TDRM). The overall process can be described as follows: First, the UAV platform collects a video sequence and feeds two adjacent frames, e.g., frame $t-1$ and frame t , into our feature extractor. Then, our ReID module augments the ReID embeddings as $\mathbf{ID}_t \in \mathbb{R}^{128 \times H \times W}$, our detection module refines the detection heatmap as $\hat{\mathbf{HM}}_t \in \mathbb{R}^{C \times H \times W}$. Here, C denotes the target category. H, W are the height and weight of the corresponding feature map. Specifically, TEBM enhances the robustness and saliency of individual embedding by combining the ReID feature map from adjacent frames. Based on the embedding inherent continuity of the tracked trajectories throughout the entire video sequence, TDRM is proposed to restore and enhance the location of targets in the detection stage.

Feature Extractor. As shown in Fig. 2, our framework adopts a weight-shared backbone (DLA-34 [10]) to get the original feature map of the previous frame $\mathbf{FM}_{t-1} \in \mathbb{R}^{64 \times H \times W}$ and current frame $\mathbf{FM}_t \in \mathbb{R}^{64 \times H \times W}$. The original feature map \mathbf{FM}_{t-1} is then passed through a separate 3×3 convolution layer, a ReLU layer and a 1×1 convolution layer to obtain the detection heatmap $\mathbf{HM}_{t-1} \in \mathbb{R}^{C \times H \times W}$ and ReID feature map $\mathbf{ID}_{t-1} \in \mathbb{R}^{128 \times H \times W}$. Also, we obtain initial results from \mathbf{FM}_t , which include ReID feature map $\mathbf{ID}_t \in \mathbb{R}^{128 \times H \times W}$, box offset of $\mathbb{R}^{2 \times H \times W}$, and box size of $\mathbb{R}^{2 \times H \times W}$.

B. Temporal Embedding Boosting Module

In the MOT system, ReID embeddings play a crucial role in online association. It generally sustains a continuous trajectory through similarity matching in adjacent frames. Nevertheless, UAV motion often introduces variations in object scale and position, which simultaneously weakens the ReID learning process and online association. To this end, we propose TEBM to enhance the ReID learning process from temporal cues.

As shown in the middle part of Fig. 2, TEBM takes the ReID feature map \mathbf{ID}_{t-1} and \mathbf{ID}_t as inputs. To obtain the statistical distribution information of the whole feature map, global average pooling (GAP) is firstly introduced to project the ReID information of the previous frame \mathbf{ID}_{t-1} as a 128-dimensional operator \mathbf{ID}_{t-1}^Q . Then we reshape the current frame $\mathbf{ID}_t \in \mathbb{R}^{128 \times H \times W}$ into $\mathbf{ID}_t^R \in \mathbb{R}^{128 \times HW}$. Lastly, we calculate the cosine similarity between the query operator \mathbf{ID}_{t-1}^Q and the key \mathbf{ID}_t^R , which can be expressed as:

$$W_c = \text{Cos}(\mathbf{ID}_{t-1}^Q, \mathbf{ID}_t^R) = \frac{\mathbf{ID}_{t-1}^Q \cdot \mathbf{ID}_t^R}{\|\mathbf{ID}_{t-1}^Q\| \cdot \|\mathbf{ID}_t^R\|} \quad (1)$$

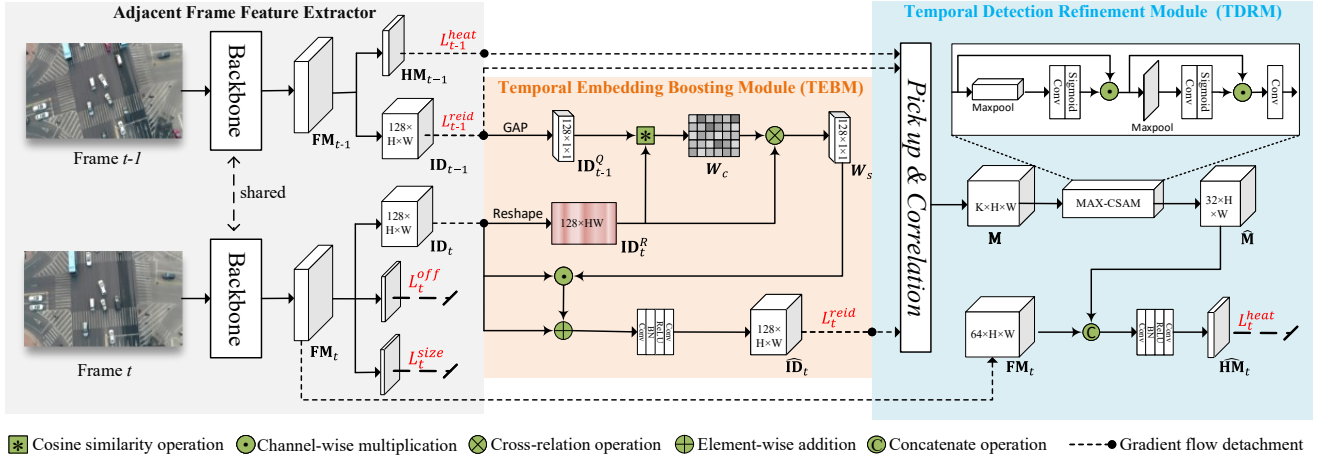


Fig. 2. Architecture details of STCMOT. It consists of three components: a Frame Feature Extractor, a Temporal Embedding Boosting Module, and a Temporal Detection Refinement Module.

Algorithm 1: Pseudo-code of Pick up & Correlation.

```

import torch
import torch.nn.function as F

def Pick_and_Corr(HM_{t-1}, ID_{t-1}, ID_t, K = 100):
    HM_{t-1}^{max} = F.maxpool_2d(HM_{t-1})
    HM_{t-1} = HM_{t-1} * (HM_{t-1} == HM_{t-1}^{max})
    HM_{t-1} = HM_{t-1}.view(-1, C*H*W)
    topK_scores, topK_inds = torch.topk(HM_{t-1}, K)
    ID_K = ID_{t-1}[topK_inds < K]
    M = torch.matmul(ID_K, ID_t)
    return M

```

where $W_c \in \mathbb{R}^{H \times W}$ is the salient attention matrix that measures the positional relationship of each instance embedding in two frames.

Following this, a cross-relation operation is employed to generate channel-level weighted descriptor W_s for the ReID feature map. Its calculation is as follows:

$$W_s = LN(Conv(ID_t^R \cdot W_c)) \quad (2)$$

where $Conv$ denotes 1×1 convolution layer while LN denotes LayerNorm layer. Finally, we employ W_s to reweight the current ReID embeddings, as depicted in Eq. 3. This approach enables the model to effectively concentrate on specific information across different channels, thus positively contributing to the extraction of discriminative embedding.

$$\hat{ID}_t = \psi(ID_t \odot W_s \oplus ID_t) \quad (3)$$

Here, \odot represents channel-wise multiplication, \oplus represents element-wise addition, and ψ denotes a Conv2d-BatchNorm-ReLU-Conv2d block used to obtain the final boosted ReID embeddings \hat{ID}_t .

C. Temporal Detection Refinement Module

Unlike single-frame detection task, the MOT system processes sequential video frames, making the temporal context information as important as spatial information. Therefore,

mining temporal trajectory information and integrating spatio-temporal features can effectively enhance MOT detection performance. As shown in the right part of Fig. 2, our TDRM is designed to fully interact with the temporal information between two adjacent frames for fine-grained detection.

The top K response probability map $M \in \mathbb{R}^{K \times H \times W}$ which generated from the *Pick up & Correlation* strategy is detailed in Algorithm 1. Specifically, we first perform a 3×3 max pooling operation on the previous heatmap HM_{t-1} and then select the top K locations of high-response points on HM_{t-1} . Afterwards, the top K embeddings $ID_K \in \mathbb{R}^{K \times 128}$ are extracted from ID_{t-1} based on their location constraint. Lastly, the probability map M is computed using the *Correlation* operator between ID_K and ID_t , which represents the likelihood that the trajectory from the previous frame is existent in the current frame.

With the probability map M , a maximum channel spatial attention module (MAX-CSAM) is used to compress the channel dimension from K to 32 to generate the aggregated similarity map \hat{M} , formatted as:

$$\hat{M} = \sigma(f_c(M_c^{max})) \odot \sigma(f_s(M_s^{max})) \odot M \quad (4)$$

where M_c^{max} and M_s^{max} are acquired through max pooling on the channel dimension and spatial dimension, respectively. f_c denotes a 1D convolution layer, f_s denotes a 7×7 convolution layer and σ is Sigmoid operator. Then, we concatenate the original feature map FM_t and \hat{M} , and pass them through a Conv2d-BatchNorm-ReLU-Conv2d block to obtain the refined detection heatmap \hat{HM}_t . It can be expressed as:

$$\hat{HM}_t = \psi([FM_t, \hat{M}]) \quad (5)$$

where $[,]$ denotes the concatenate operation. The final detection heatmap \hat{HM}_t fuses prior trajectory information to increase the probability of target appearance and focuses on reducing missed detections.

D. Objective Function

With the consecutive frame pipeline, joint loss functions are employed to supervise the model training process. As depicted

TABLE I
QUANTITATIVE COMPARISON WITH THE EXISTING STATE-OF-THE-ART METHODS ON VISDRONE2019 AND UAVDT TEST SETS.

Dataset	Method	Pub&Year	IDF1↑ (%)	MOTA↑ (%)	MT↑	ML↓	FP↓	FN↓	IDS↓
VisDrone2019	SORT [16]	ICIP2016	38.0	14.0	506	545	80845	112954	3629
	IOU [17]	AVSS2017	38.9	28.1	467	670	36158	126549	2393
	MOTR [18]	ECCV2022	41.4	22.8	272	825	28407	147937	959
	TrackFormer [19]	CVPR2022	30.5	25.0	385	770	25856	141526	4840
	ByteTrack [4]	ECCV2022	37.0	35.7	-	-	21434	124042	2168
	UAVMOT [15]	CVPR2022	51.0	36.1	520	574	27983	115925	2775
	OCSORT [5]	CVPR2023	50.4	39.6	-	-	14631	123513	986
	STCMOT Ours	Ours	52.0	41.2	667	453	36428	94445	3984
UAVDT	SORT [16]	ICIP2016	43.7	39.0	484	400	33037	172628	2350
	IOU [17]	AVSS2017	23.7	36.6	534	357	42245	163881	9938
	DSORT [3]	ICIP2017	58.2	40.7	595	358	44868	155290	2061
	ByteTrack [4]	ECCV2022	59.1	41.6	-	-	28819	189197	296
	UAVMOT [15]	CVPR2022	67.3	46.4	624	221	66352	115940	456
	OCSORT [5]	CVPR2023	64.9	47.5	-	-	47681	148378	288
	STCMOT Ours	Ours	69.8	49.2	664	203	72901	99547	665

in Fig. 2, the previous frame $t - 1$ is supervised with ReID loss L_{t-1}^{reid} and heatmap loss L_{t-1}^{heat} . Meanwhile, the current frame t produces ReID loss L_t^{reid} along with detection losses, including heatmap loss L_t^{heat} , offset loss L_t^{off} , and size loss L_t^{wh} .

Following CenterNet [10], we use the L1 loss function to supervise L_t^{off} and L_t^{wh} , and apply the focal loss function to supervise L_{t-1}^{heat} and L_t^{heat} . In terms of ReID loss, we consider each instance as a distinct class and transform the predicted feature map into a class distribution vector $\mathbf{P} = \{p_i\}_i^N$ using a fully connected layer and a softmax operation. Here, N is the number of all targets in the training set. The one-hot representation of the ground-truth label can be denoted as $\mathbf{Q} = \{q_i\}_i^N$, then the cross-entropy loss function is employed to supervise the ReID loss between \mathbf{P} and \mathbf{Q} . The overall loss can be expressed as:

$$L = \frac{1}{2} \left[\frac{1}{e^{\beta_1}} (L_{t-1}^{heat} + L_t^{heat} + L_t^{off} + L_t^{wh}) + \frac{1}{e^{\beta_2}} (L_{t-1}^{reid} + L_t^{reid}) \right] + \beta_1 + \beta_2 \quad (6)$$

where β_1 and β_2 represent learnable coefficients in [20] to balance different branches.

III. EXPERIMENTS

A. Implementation Details

During training, the raw frames are resized into $3 \times 608 \times 1088$ pixels as inputs for the feature extractor to generate the original feature map $\mathbf{FM} \in \mathbb{R}^{64 \times H \times W}$, where $H = 152$ and $W = 272$. We adopt the Adam optimizer with an initial learning rate of $7e-5$ to train our network. The batch size is set to 16. There are a total of 30 epochs while the learning rate decays to $7e-6$ after 20 epochs. To obtain temporal trajectory information, we randomly sample frame pairs from the same video sequences under the condition that the interval between these sample pairs is within 3 frames. All experiments in this work are implemented with four NVIDIA GeForce RTX 3090 GPUs.

B. Online Inference

In the inference phase, we follow the online data association pipeline in ByteTrack [4]. Specifically, we classify the detection results into high-confidence and low-confidence detections based on a specified threshold $\tau = 0.4$. In high-confidence detection cases, we first utilize the Kalman filter to predict the location of each trajectory and compute the Mahalanobis distance between the current detections and the predicted trajectories. The cosine distance computed on ReID embeddings is then combined with the Mahalanobis distance to complete the initial matching. Subsequently, the remaining detections and trajectories are matched by intersection over union (IOU) distance. In low-confidence detection cases, we directly employ IOU distance to associate unmatched trajectories and recover low-scoring detection boxes. Finally, we initialize unmatched high-confidence detections as new trajectories while discarding unmatched low-confidence results. The last remaining unmatched trajectories are stored for 30 frames.

C. Comparison with State of the Arts

We evaluate our proposed STCMOT with current state-of-the-art MOT methods in two datasets: VisDrone2019 [21] and UAVDT [22]. In Table I, multiple metrics [23] are presented to assess tracking performance. Among them, MOTA and IDF1 are key metrics, which emphasize detection performance and association performance, respectively.

Results on VisDrone2019: VisDrone2019 is a fundamental benchmark for multiple object tracking based on UAV-captured videos. It contains 10 categories, including pedestrians, vehicles, etc. Table I demonstrates that STCMOT achieves a new state-of-the-art performance with 52.0% on IDF1 and 41.2% on MOTA, outperforming all the previous outstanding trackers. Concretely, our method outperforms UAVMOT [15] by 1.0% on IDF1 and 5.1% on MOTA. Compared with OCSORT [5], our method improves IDF1 and MOTA by 1.6% and 1.6%, respectively.

Results on UAVDT: The tracking videos in UAVDT are derived from bird's-eye views at different altitudes and diverse

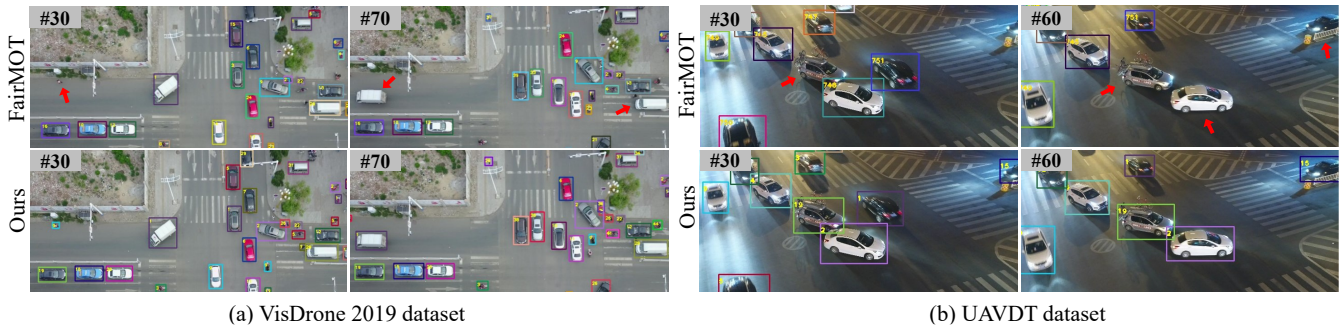


Fig. 3. Visualization of our STCMOT and baseline FairMOT on the VisDrone2019-uav0305 set and UAVDT-M0205 sets. Each bounding box with a unique ID number represents a tracked target.

outdoor scenes. The tracking results of UAVDT are shown in Table I. We can observe that STCMOT shows the best tracking performance with 69.8% on IDF1 and 49.2% on MOTA. In particular, STCMOT improves UVMOT [15] by 2.5% on IDF1 and 2.8% on MOTA, while outperforming OCSORT [5] by 4.9% on IDF1 and 1.7% on MOTA.

D. Ablation Study

To validate the effectiveness of the individual components of our proposed tracking framework, we conduct ablation experiments on the VisDrone2019 test set. Note that FairMOT [8] is set as our baseline method.

Component ablation. As shown in Table II, when combining baseline with our proposed TEBM, the performance improves by 4.1% on IDF1 and 4.2% on MOTA. While combining baseline with the TDRM, we achieve 51.0% on IDF1 and 38.5% on MOTA, respectively. These showcase their respective contributions to the final STCMOT. Further, there is a mutually reinforcing improvement (+5.8% on IDF1 and +5.5% on MOTA) in final performance when using TEBM and TDRM together.

Attributes performance ablation. To investigate the contribution of the proposed modules, we evaluate the identification precision (IDP) and identification recall (IDR) w.r.t. association performance, as well as precision and recall w.r.t. detection performance. The results of these comparisons are presented in Table III. As we can see, TEBM contributes most to the IDP/Precision attributes while TDRM contributes mainly to IDR (+7.1%) and Recall (+7.5%). This indicates that TEBM is primarily geared towards enhancing the accuracy of target identification, whereas TDRM exhibits a more robust capability in capturing targets. In addition, TEBM has achieved significant improvements in all four specific metrics. This phenomenon shows that TEBM effectively strengthens the data association ability and demonstrates its superiority in comprehensive performance. In contrast to the baseline, TDRM shows a lower Precision. This is mainly attributed to the trade-off between reducing the number of missed detections and an increase in false positives. However, TDRM has significantly enhanced performance compared with the baseline in terms of both IDF1 and MOTA metrics, serving as compelling evidence of its effectiveness.

TABLE II
COMPONENTS ABLATION RESULTS.

TEBM	TDRM	IDF1↑ (%)	MOTA↑ (%)	MT↑	ML↓	FP↓	FN↓	IDS↑
		46.2	35.7	509	532	29241	114286	4152
✓		50.3(+4.1)	39.9(+4.2)	574	503	27721	106176	4045
	✓	51.0(+4.8)	38.5(+2.8)	653	475	40113	97105	3836
✓	✓	52.0(+5.8)	41.2(+5.5)	667	453	36428	94445	3984

TABLE III
THE IMPACT OF COMPONENTS ON SPECIFIC ASSOCIATION AND DETECTION METRICS.

Module	IDP↑ (%)	IDR↑ (%)	Precision↑ (%)	Recall↑ (%)
Base	59.8	37.6	79.8	50.2
Base+TEBM	63.4(+3.6)	41.7(+4.1)	81.7(+1.9)	53.7(+4.1)
Base+TDRM	59.5(-0.3)	44.7(+7.1)	76.8(-3.0)	57.7(+7.5)

E. Visualization and Analysis

In this subsection, we qualitatively analyze the robustness of STCMOT under challenging scenarios. As depicted in Fig. 3 (a), when faced with targets of similar appearance and small size, the FairMOT [8] fails to track them within a certain interval, while our STCMOT can maintain the continuity of their trajectories. The relative motion between the vehicles and the UAV platform causes target deformation and blurring, as illustrated in Fig. 3 (b). FairMOT misses these vehicles, but our STCMOT can accurately track them. In general, FairMOT encounters difficulty in tracking targets under extreme scenarios, as indicated by the red arrows in the failure cases. On the contrary, our method successfully tracks these targets across multiple frames and consistently preserves their unique identity numbers. Moreover, as shown in Fig. 1, compared with FairMOT, STCMOT exhibits superior discriminative embedding representation, particularly in scenarios where targets have similar appearances. These visualizations reveal the adaptability of our STCMOT to complex scenarios in UAV videos, which exploits spatial and temporal information to achieve more robust and accurate tracking results.

IV. CONCLUSION

In this paper, we propose a novel spatio-temporal feature cohesion framework for the UAV-based MOT task, which considers the sequence temporal consistency for both ReID and detection branches. For the ReID branch, we introduce the temporal embedding boosting module (TEBM), which assesses the similarity among adjacent ReID feature maps to enhance the distinctiveness of individual embedding features.

For the detection branch, the temporal detection refinement module (TDRM) is proposed to propagate trajectory embedding and prominently highlight potential target positions. Experiments demonstrate that our proposed STCMOT can effectively mitigate the occurrence of missed targets and improve tracking consistency. Moreover, STCMOT achieves new state-of-the-art performance on popular UAV-based MOT benchmarks. In particular, it realizes an IDF1 of 52.0% and a MOTA of 41.2% on the VisDrone2019 dataset, and an IDF1 of 69.3% and a MOTA of 48.9% on the UAVDT dataset, respectively.

REFERENCES

- [1] Xin Wu, Wei Li, Danfeng Hong, Ran Tao, and Qian Du, "Deep learning for unmanned aerial vehicle-based object detection and tracking: A survey," *IEEE Geoscience and Remote Sensing Magazine*, vol. 10, no. 1, pp. 91–124, 2022.
- [2] Long Chen, Haizhou Ai, Zijie Zhuang, and Chong Shang, "Real-time multiple people tracking with deeply learned candidate selection and person re-identification," in *2018 IEEE International Conference on Multimedia and Expo (ICME)*, 2018, pp. 1–6.
- [3] Nicolai Wojke, Alex Bewley, and Dietrich Paulus, "Simple online and realtime tracking with a deep association metric," in *2017 IEEE international conference on image processing (ICIP)*, 2017, pp. 3645–3649.
- [4] Yifu Zhang, Peize Sun, Yi Jiang, Dongdong Yu, Fucheng Weng, Zehuan Yuan, Ping Luo, Wenyu Liu, and Xinggang Wang, "Bytetrack: Multi-object tracking by associating every detection box," in *European Conference on Computer Vision*. Springer, 2022, pp. 1–21.
- [5] Jinkun Cao, Jiangmiao Pang, Xinshuo Weng, Rawal Khirodkar, and Kris Kitani, "Observation-centric sort: Rethinking sort for robust multi-object tracking," in *Proceedings of the IEEE/CVF Conference on Computer Vision and Pattern Recognition*, 2023, pp. 9686–9696.
- [6] Nir Aharon, Roy Orfaig, and Ben-Zion Bobrovsky, "Bot-sort: Robust associations multi-pedestrian tracking," *ArXiv*, vol. abs/2206.14651, 2022.
- [7] Zhongdao Wang, Liang Zheng, Yixuan Liu, Yali Li, and Shengjin Wang, "Towards real-time multi-object tracking," in *European Conference on Computer Vision*. Springer, 2020, pp. 107–122.
- [8] Yifu Zhang, Chunyu Wang, Xinggang Wang, Wenjun Zeng, and Wenyu Liu, "Fairmot: On the fairness of detection and re-identification in multiple object tracking," *International Journal of Computer Vision*, vol. 129, pp. 3069–3087, 2021.
- [9] Yan Jin, Fang Gao, Jun Yu, Jiabao Wang, and Feng Shuang, "Multi-object tracking: Decoupling features to solve the contradictory dilemma of feature requirements," *IEEE Transactions on Circuits and Systems for Video Technology*, vol. 33, no. 9, pp. 5117–5132, 2023.
- [10] Xingyi Zhou, Dequan Wang, and Philipp Krähenbühl, "Objects as points," *arXiv preprint arXiv:1904.07850*, 2019.
- [11] Han Wu, Jiahao Nie, Zhiwei He, Ziming Zhu, and Mingyu Gao, "One-shot multiple object tracking in uav videos using task-specific fine-grained features," *Remote Sensing*, vol. 14, no. 16, 2022.
- [12] Han Wu, Zhiwei He, and Mingyu Gao, "Gcevt: Learning global context embedding for vehicle tracking in unmanned aerial vehicle videos," *IEEE Geoscience and Remote Sensing Letters*, vol. 20, pp. 1–5, 2023.
- [13] En Yu, Zhuoling Li, Shoudong Han, and Hongwei Wang, "Relationtrack: Relation-aware multiple object tracking with decoupled representation," *IEEE Transactions on Multimedia*, 2022.
- [14] Chao Liang, Zhipeng Zhang, Xue Zhou, Bing Li, Shuyuan Zhu, and Weiming Hu, "Rethinking the competition between detection and reid in multiobject tracking," *IEEE Transactions on Image Processing*, vol. 31, pp. 3182–3196, 2022.
- [15] Shuai Liu, Xin Li, Huchuan Lu, and You He, "Multi-object tracking meets moving uav," in *Proceedings of the IEEE/CVF Conference on Computer Vision and Pattern Recognition*, 2022, pp. 8876–8885.
- [16] Alex Bewley, Zongyuan Ge, Lionel Ott, Fabio Ramos, and Ben Uppcroft, "Simple online and realtime tracking," in *2016 IEEE international conference on image processing (ICIP)*. IEEE, 2016, pp. 3464–3468.
- [17] Erik Bochinski, Volker Eiselein, and Thomas Sikora, "High-speed tracking-by-detection without using image information," in *2017 14th IEEE International Conference on Advanced Video and Signal Based Surveillance (AVSS)*, 2017, pp. 1–6.
- [18] Fangao Zeng, Bin Dong, Yuang Zhang, Tiancai Wang, Xiangyu Zhang, and Yichen Wei, "Motr: End-to-end multiple-object tracking with transformer," in *European Conference on Computer Vision*. Springer, 2022, pp. 659–675.
- [19] Tim Meinhardt, Alexander Kirillov, Laura Leal-Taixe, and Christoph Feichtenhofer, "Trackformer: Multi-object tracking with transformers," in *Proceedings of the IEEE/CVF conference on computer vision and pattern recognition*, 2022, pp. 8844–8854.
- [20] Alex Kendall, Yarin Gal, and Roberto Cipolla, "Multi-task learning using uncertainty to weigh losses for scene geometry and semantics," in *Proceedings of the IEEE conference on computer vision and pattern recognition*, 2018, pp. 7482–7491.
- [21] Dawei Du, Pengfei Zhu, Longyin Wen, Xiao Bian, Haibin Lin, Qinghua Hu, Tao Peng, Jiayu Zheng, Xinyao Wang, Yue Zhang, et al., "Visdrone-det2019: The vision meets drone object detection in image challenge results," in *Proceedings of the IEEE/CVF international conference on computer vision workshops*, 2019, pp. 0–0.
- [22] Dawei Du, Yuankai Qi, Hongyang Yu, Yifan Yang, Kaiwen Duan, Guorong Li, Weigang Zhang, Qingming Huang, and Qi Tian, "The unmanned aerial vehicle benchmark: Object detection and tracking," in *Proceedings of the European conference on computer vision (ECCV)*, 2018, pp. 370–386.
- [23] Anton Milan, Laura Leal-Taixé, Ian Reid, Stefan Roth, and Konrad Schindler, "Mot16: A benchmark for multi-object tracking," *arXiv preprint arXiv:1603.00831*, 2016.